ChemPubSoc Europe
DOI: 10.1002/cphc.201500885
CHEMPHYSCHEM Articles

The Nature of the Singlet and Triplet States of Cyclobutadiene as Revealed by Quantum Interference

Felipe Fantuzzi, Thiago M. Cardozo, and Marco A. C. Nascimento*[a]

The generalized product function energy partitioning (GPF-EP) method is applied to the description of the cyclobutadiene molecule. The GPF wave function was built to reproduce generalized valence bond (GVB) and spin-coupled (SC) wave functions. The influence of quasiclassical and quantum interference contributions to each chemical bond of the system are analyzed along the automerization reaction coordinate for the lowest singlet and triplet states. The results show that the interference effect on the π space reduces the electronic energy of the singlet cyclobutadiene relative to the second-order Jahn–Teller distortion, which takes the molecule from a D_{4h} to a D_{2h} structure. Our results also suggest that the π space of the $^1B_{1g}$ state of the square cyclobutadiene is composed of a weak four center–four electron bond, whereas the $^3A_{2g}$ state has a four center–two electron π bond. Finally, we also show that, although strain effects are nonnegligible, the thermodynamics of the main decomposition pathway of cyclobutadiene in the gas phase is dominated by the π space interference.

1. Introduction

Cyclobutadiene is one of the most intriguing systems in chemistry. For many decades it has been the focus of a great diversity of experimental[1–10] and theoretical[11–36] studies. Despite its apparently simple electronic structure, interesting and unexpected features have been identified since the early works.[37–42] Although it is widely accepted that the majority of its peculiar properties are due to a combination between electronic (antiaromaticity) and structural (high angular strain) effects, their relative contributions and origins are still subjects of research.[43–45]

At the end of the 1960s, the amount of accumulated knowledge of experimental aspects of cyclobutadiene derivatives was large enough to make up an entire book.[46] However, the lack of information about the parent molecule has led to the conclusion that it should react as triplet diradicals. It was the pioneering synthesis of Dewar benzene derivatives from the decomposition of cyclobutadiene–iron tricarbonyl complexes, developed by Pettit and co-workers,[37] that completely changed this scenario. There were evidences that cyclobutadiene was generated in situ, and its reactivity led the authors to question the nature of the ground-state spin multiplicity of the system.[37–40] Inspired by the work of Pettit and co-workers, Dewar and Gleicher addressed a theoretical study on the molecule and concluded that the ground state should have a singlet multiplicity and a rectangular geometry.[38] The excited triplet state, on the other hand, was characterized as a squared geometry with a large negative resonance energy.

[a] F. Fantuzzi, Dr. T. M. Cardozo, Prof. Dr. M. A. C. Nascimento
Instituto de Química
Universidade Federal do Rio de Janeiro
Centro de Tecnologia, Bloco A sala 412
Rio de Janeiro, RJ 21.941-909, (Brazil)
E-mail: chaer01@gmail.com

In the following decades, several experiments and calculations confirmed the hypothesis developed by the groups of Pettit and Dewar.[47] It was also commonly accepted that the singlet square geometry is a saddle point for automerization of the two rectangular structures.[14,47] However, the relative energy of the lowest singlet and triplet states at the square geometry was somewhat controversial. Molecular orbital (MO) methods wrongly predicted a lower energy triplet state at that structure,[24,25] whereas modern valence bond methods, such as generalized valence bond (GVB) and spin-coupled (SC), correctly described the ordering of the states.[26,27] In fact, the failure of the MO methods to describe the square ground state is considered an example of a violation of Hund's rule, owing to a dynamic spin polarization mechanism, which lowers the energy of a singlet state (compared with the triplet state) in a biradical species through a configuration interaction (CI).[27,48,49] It is now well-established by high level ab initio calculations that the singlet–triplet energy gap between the X^1B_{1g} and the $^3A_{2g}$ states ranges from 10 to 14 kcal mol^{-1}.[32]

Concerning the automerization reaction, the energy barrier for the interconversion between two equivalent D_{2h} structures at the singlet ground state was experimentally predicted to be in the range of 1.6–10 kcal mol^{-1}.[50] Owing to this large span of the experimental values, Eckert-Maksić et al.[34] employed the high-level multireference average-quadratic coupled cluster method to study this reaction and discriminate between the measured data. They found an energy barrier of 6.3 kcal mol^{-1}, which includes both electronic and zero-point vibrational energy contributions. Moreover, experimental evidences suggested that the two rectangular isomers of cyclobutadiene and its deuterated derivatives undergo a rapid flipping interconversion even at 10 K.[8] A heavy-atom tunneling hypothesis was proposed by Carpenter and Whitman as the main mechanism of the automerization reaction.[50,51] Although this mechanism

was tested experimentally and theoretically, to the best of our knowledge, a final conclusion about its validity has yet to be reached.[52–55]

The distortion of the singlet ground state from a square to a rectangular structure can be understood as the result of a second-order Jahn–Teller effect. According to Pearson,[56] if the integral $\langle \Psi_0 | \partial H/\partial Q | \Psi_e \rangle$, in which Ψ_0 is the ground state and Ψ_e is a low-lying electronic state, is nonzero, then a distortion might occur along the coordinate $\vec{Q}$. In other words, if the direct product of the symmetry representations of $\vec{Q}$ and Ψ_e contains the symmetry representation of Ψ_0, a distortion along $\vec{Q}$ might happen. This is exactly the case for the excited $^1A_{1g}$ state and the b_{1g} vibration (rectangular distortion). As a consequence, the mixing of both singlet states along the b_{1g} mode of vibration lowers the energy.[27]

The second-order Jahn–Teller distortion can also be analyzed in terms of bonding of the σ and π electrons. It was proposed by Shaik et al.,[19] and supported by other studies,[36] that π electrons in alternated bonds possess a distortive propensity, favoring structures with localized double bonds. In fact, the low energy and large amplitude properties of the b_{2u} vibrational mode of benzene, which was experimentally observed by Berry in 1961,[57] are evidences of such an effect. Thus, the equilibrium geometry of aromatic and antiaromatic molecules would be a balance between the strength of the covalent π distortive effect, the tendency of the σ electrons to counteract the distortive trend, and quasiclassical effects.[58]

In this work, the chemical bonding of the lowest singlet and triplet states of cyclobutadiene is analyzed along the automerization reaction coordinate. The generalized product function energy partitioning (GPF-EP) method is used to highlight the chemical structure of the π space of the square and rectangular minimum geometries, and to analyze the quantum interference effect along the distortion.[59] It is known that interference is responsible for the formation of chemical bonds, and this effect can be quantified within the GPF-EP approach for each individual chemical bond in diatomic or polyatomic systems.[58–65] Finally, to highlight the main factors that contribute to the low thermodynamic stability of cyclobutadiene, the interference contribution is analyzed along the main decomposition reaction of the molecule in the gas phase.

Computational Details

The geometries of the square $^1B_{1g}$ and $^3A_{2g}$ states, as well as the rectangular ^1A_g state, of cyclobutadiene were optimized at the multiconfigurational complete active space self-consistent field (CASSCF) level.[66–68] The four π electrons were distributed between all configurations that were constructed from four molecular orbitals, built from the Dunning double-zeta correlation-consistent basis set, cc-pVDZ.[69] Single-point calculations, applying generalized product functions (GPF), were performed for the singlet and triplet states along the automerization vector $\vec{Q}$. The GPF-EP method was used to evaluate the chemical structure and the nature of the chemical bonding of the systems. The method was derived by applying the partitioning scheme developed by Ruedenberg to GPF wave functions constructed with modern valence bond group functions.[70] The general form of a GPF wave function, as defined by McWeeny,[71] is shown in Equation (1):

$$\Psi_{GPF} = \hat{A}\{\psi_1\psi_2\cdots\psi_N\} \tag{1}$$

where $\hat{A}$ is the antisymmetrizer operator, and the indexes 1 and 2 represent different orthogonal wave functions (groups).

The strong orthogonality condition is imposed to each group, in the same way that the generalized valence bond (GVB) orbital pairs in the perfect-pairing (GVB-PP) wave function. However, groups can be described with different methods in the GPF wave function, and more than two electrons can be inserted in a single group. In this work, all electrons belonging to the core were embedded into one group, and treated at the restricted Hartree–Fock (RHF) level. As the core electrons play a smaller role in chemical bonding, this can be considered a reasonable approximation. In contrast, all valence electrons were described using modern valence bond methods. A GVB-PP group was defined for each pair of σ electrons, whereas the four π electrons were inserted into one group and characterized using a full GVB or, equivalently, a spin-coupled wave function.

Only a brief discussion of the GPF-EP method will be presented. Detailed information can be found elsewhere.[59]

The first- and second-order reduced density matrices (RDM-1 and RDM-2) for GPF wave functions are as follows [Eqs. (2a) and (2b)]:

$$\rho(\vec{r}_1,\vec{r}'_1) = \sum_{\mu=1}^{\eta}\rho^{\mu}(\vec{r}_1,\vec{r}'_1) \tag{2a}$$

$$\pi(\vec{r}_1\vec{r}_2,\vec{r}'_1\vec{r}'_2) = \sum_{\mu=1}^{\eta}\pi^{\mu}(\vec{r}_1\vec{r}_2,\vec{r}'_1\vec{r}'_2) + \frac{1}{2}\sum_{\mu=1}^{\eta}\sum_{\nu>\mu}^{\eta}\left[\rho^{\mu}(\vec{r}_1,\vec{r}'_1)\rho^{\nu}(\vec{r}_2,\vec{r}'_2) - \frac{1}{2}\rho^{\mu}(\vec{r}_2,\vec{r}'_1)\rho^{\nu}(\vec{r}_1,\vec{r}'_2)\right] \tag{2b}$$

where η is the number of groups in the GPF function. In terms of the reduced density matrices, the total electronic energy expression for a GPF wave function is [Eq. (3)]:

$$\begin{aligned} E_{GPF} = {} & \sum_{\mu=1}^{\eta}\left\{\int\left[\hat{h}\rho^{\mu}(\vec{r}_1,\vec{r}'_1)\right]_{\vec{r}_1=\vec{r}'_1}d\vec{r}_1 + \frac{1}{2}\iint\left[\frac{\pi^{\mu}(\vec{r}_1\vec{r}_2,\vec{r}'_1\vec{r}'_2)}{r_{12}}\right]_{\substack{\vec{r}_1=\vec{r}'_1\\ \vec{r}_2=\vec{r}'_2}}d\vec{r}_1d\vec{r}_2\right\} + \\ & \frac{1}{2}\sum_{\mu=1}^{\eta}\sum_{\nu\neq\mu}^{\eta}\left\{\frac{1}{2}\iint\left[\frac{\rho^{\mu}(\vec{r}_1,\vec{r}'_1)\rho^{\nu}(\vec{r}_2,\vec{r}'_2)}{r_{12}}\right]_{\substack{\vec{r}_1=\vec{r}'_1\\ \vec{r}_2=\vec{r}'_2}}d\vec{r}_1d\vec{r}_2\right\} - \\ & \frac{1}{2}\sum_{\mu=1}^{\eta}\sum_{\nu\neq\mu}^{\eta}\left\{\frac{1}{4}\iint\left[\frac{\rho^{\mu}(\vec{r}_2,\vec{r}'_1)\rho^{\nu}(\vec{r}_1,\vec{r}'_2)}{r_{12}}\right]_{\substack{\vec{r}_1=\vec{r}'_1\\ \vec{r}_2=\vec{r}'_2}}d\vec{r}_1d\vec{r}_2\right\} + \\ & \sum_{A=1}^{M}\sum_{B>A}^{M}\frac{Z_AZ_B}{r_{AB}} \end{aligned} \tag{3}$$

where $\hat{h}$ is the one-electron operator, which includes both kinetic energy and electron-nuclei potential energy. The expression in the first bracket is the intragroup energy, whereas the remaining parts of Equation (3) are the Coulomb and exchange intergroup contributions. The GPF-EP method splits both ρ and π into interference and reference (quasiclassical) densities, in which the latter involves the sum of quasiclassical densities. For a single group, the quasi-

classical (ρ_{QC}) and interference (ρ_I) densities are [Eqs. (4) and (5)]:

$$\rho_{QC}^{\mu} = \sum_{r=1}^{N^{\mu}} \left[\phi_r^{\mu}(\vec{r})\right]^2 \tag{4}$$

$$\rho_I^{\mu} = \sum_{r,s}{}' \langle r,s\rangle^{\mu} p(r|s) \tag{5}$$

where μ is the selected group index, N^{μ} is the number of electrons in this group, $p(r|s)$ are the density matrix elements expressed in the orbital basis set, and $<r,s>^{\mu}$ is the interference density for orbitals ϕ_r an ϕ_s [Eq. (6)]:

$$\langle r,s\rangle^{\mu} = \phi_r^{\mu}(\vec{r})\phi_s^{\mu}(\vec{r}) - \frac{1}{2}\xi(r,s)\left\{\left[\phi_r^{\mu}(\vec{r})\right]^2 + \left[\phi_s^{\mu}(\vec{r})\right]^2\right\} \tag{6}$$

where $\xi(r,s)$ is the overlap integral between ϕ_r^{μ} and ϕ_s^{μ}. The total energy of the system can be separated as follows [Eq. (7)]:

$$E[\text{tot}] = E[\text{ref}] + E[x] + E[\text{I}] + E[\text{II}] \tag{7}$$

where E[ref] is the total reference energy, E[I] and E[II] are the first and second-order interference energies, and $E[x]$ is the total intergroup exchange energy, which comes from the antisymmetrization of the GPF wave function. The $E[x]$ term would not exist if the GPF wave function consisted of a single group. Consequently, it merely represents a symmetry correction to the reference energy, due to the separation of the total wave function into different groups. In Equation (7), the sum E[ref]$+E[x]$ corresponds to the quasiclassical contribution, E[ref$+x$], and E[I]$+E$[II] is the total interference contribution, E[I$+$II].

The E[ref] and E[I] terms can be separated into kinetic (T[ref] and T[I]), electron-electron potential (V_{ee}[ref] and V_{ee}[I]) and electron-nuclei (V_{en}[ref] and V_{en}[I]) energies. On the other hand, the E[II] term consists entirely of electron-electron repulsion terms, and can be equivalently referred to as V_{ee}[II]. The energy terms can also be divided into intragroup and intergroup contributions, as follows [Eqs. (8 a)–(8 d)]:

$$E[\text{ref}] = \sum_{\mu=1}^{\eta} E^{\mu}[\text{ref}] + \sum_{\mu<\nu}^{\eta} E^{\mu,\nu}[\text{ref}] \tag{8a}$$

$$E[\text{I}] = \sum_{\mu=1}^{\eta} E^{\mu}[\text{I}] \tag{8b}$$

$$E[\text{II}] = \sum_{\mu=1}^{\eta} E^{\mu}[\text{II}] + \sum_{\mu<\nu}^{\eta} E^{\mu,\nu}[\text{II}] \tag{8c}$$

$$E[x] = \sum_{\mu<\nu}^{\eta} E^{\mu,\nu}[x] \tag{8d}$$

The CASSCF calculations were performed with the GAMESS program.[72] The GPF wave functions were constructed and optimized with the VB2000 package.[73] To maintain the σ–π separation approximation, Jacobi rotations for the orbitals of the π bonds and the ones belonging to the σ bonds were disabled. A stand-alone code was developed to obtain the GPF-EP.

2. Results and Discussion

Before going into the details of the interference calculations, it would be instructive to compare the shape of the spin-coupled π space orbitals of the $^1B_{1g}$ state of the square cyclobutadiene, with those obtained by Gerratt et al. and McWeeny[26,74] Figure 1 shows two different sets of orbitals, as solutions for the singlet ground-state structure. The first set (Figure 1 a) is composed of four p-like type orbitals, equally polarized to both adjacent centers. These orbitals resemble the shape of the Spin-coupled orbitals of the π space of benzene, and are chemically intuitive, that is, they bear relation to the classical valence bond picture. In contrast, the second set of orbitals (Figure 1 b) is remarkably different from what one should obtain in a classical valence bond description. The orbitals $\phi_{++,a}$ and $\phi_{++,b}$ are composed of a combination of p-like basis functions with the same sign centered on nonadjacent carbon atoms. $\phi_{+-,a}$ and $\phi_{+-,b}$ are also composed by a combination of p-like basis functions on nonadjacent carbon atoms, but with opposite signs. This set of orbitals, named "antipair" orbitals, has already been described by Gerratt et al. and McWeeny[26,74] These authors[26,74] concluded that the difference in energy between both descriptions is so small that these different sets could be characterized as equally valid descriptions. The reason for this peculiar behavior is related to the symme-

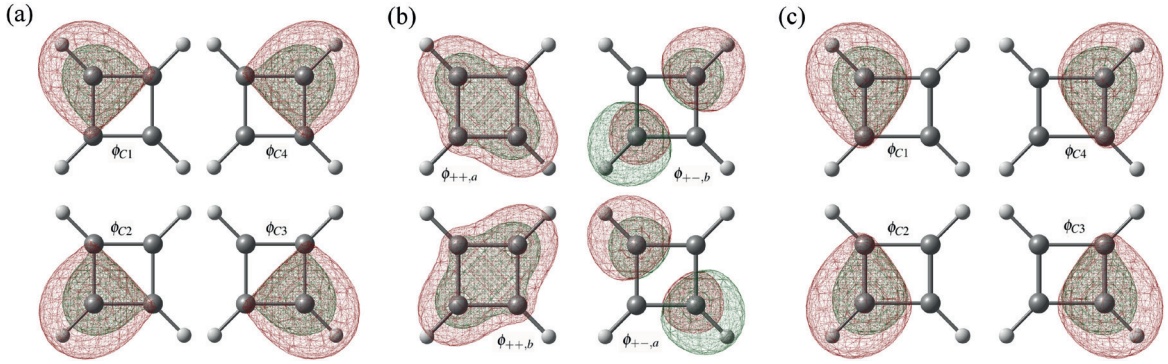

Figure 1. Spin-Coupled orbitals of the π space of the $^1B_{1g}$ square cyclobutadiene. a) Localized Orbitals. Top left: orbital ϕ_{C1}; bottom left: orbital ϕ_{C2}; bottom right: orbital ϕ_{C3}; top right: orbital ϕ_{C4}. b) Antipair Orbitals. Top left: orbital $\phi_{++,a}$; bottom left: orbital $\phi_{++,b}$; bottom right: orbital $\phi_{+-,a}$; top right: orbital $\phi_{+-,b}$. c) Orbitals for the D_{2h} global minimum structure.

try of the state. With localized p-like orbitals, the π electrons associated with nonadjacent centers must be almost orthogonal, because of symmetry considerations. The two subsets of quasitriplet couplings are combined to form a singlet state. In this case, the spin-coupled wave function does not change if a new set of orbitals is built from the sum and from the difference between the nonadjacent orbitals, which transforms the localized orbitals into antipair orbitals. For the triplet square state, only the set of antipair orbitals was found. The orbitals are identical to the ones shown in Figure 1 b.

In Figure 1 c, the spin-coupled orbitals of the π space of the global minimum X^1A_g rectangular cyclobutadiene are shown. In this case, it is possible to see that the orbitals are also p-like in nature, but there are differences in the shape compared with the localized square singlet orbitals. Rather than equally polarized, after the second-order Jahn–Teller distortion each orbital is more polarized to the closest adjacent center. As these orbitals are localized in nature, and the descriptions for the singlet square are equivalent, the set of localized orbitals were employed to describe the $^1B_{1g}$ state of cyclobutadiene in terms of energy partitioning and interference contributions.

In Section 2.1, the role of interference on the nature of the chemical bond in cyclobutadiene is analyzed. Section 2.2 shows the energy partitioning along the automerization reaction. Finally, in Section 2.3, a simple analysis of the interference contribution to the thermodynamics of the gas-phase decomposition of cyclobutadiene is presented.

2.1. Interference Energy and the Nature of the Chemical Bond in Cyclobutadiene

Table 1 shows the calculated total energy and the energy partitioning into interference and quasiclassical contributions for the singlet rectangle cyclobutadiene global minimum structure (X^1A_g); the triplet square cyclobutadiene minimum geometry ($^3A_{2g}$); and for the singlet-state square geometry ($^1B_{1g}$). One can see that the energy difference between the rectangle and the square singlet cyclobutadiene is 0.0116 Ha (7.3 kcal mol^{-1}), which is in agreement with previous studies. Moreover, at the square geometry the $^1B_{1g}$ state is 0.0161 Ha (10.1 kcal mol^{-1}) more stable than the $^3A_{2g}$ state, also corroborating with results obtained by other groups.[34]

Important differences between the systems can be identified by analysis of the energy partitioning terms. For the square cyclobutadiene, the exchange energy term, $E[x]$, is similar in both states; however, there is a stabilization of 0.2857 Ha (179.3 kcal mol^{-1}) for the $^1B_{1g}$ state by the reference contribution E[ref]. This energy difference is balanced by the E[II] term, which favors the stabilization of the triplet state by 0.2325 Ha (145.9 kcal mol^{-1}). In fact, the $^3A_{2g}$ square cyclobutadiene is the first case studied by our group in which the absolute value of the second-order interference contribution presents such a large relevance. Further analyses have shown that this contribution is associated to the exchange energy between the two antipairs of the SC group. As, by definition, the $E[x]$ contribution contains only intergroup terms, this quantity appears as an intragroup E[II] term of the spin-coupled group.; this happens because the description of the two antipairs of the orbitals cannot be obtained if each pair is placed in a different SC group. However, this contribution is not covalent in nature, and therefore will not be discussed in the following sections. On the other hand, the E[I] term is more negative for the triplet square cyclobutadiene than for the singlet state. This indicates that covalent effects in the π space are more prominent in the triplet state.

Comparing the singlet square and rectangular cyclobutadienes, it is possible to see that although the sum of reference and exchange energies (the corrected quasiclassical energy) favors the stabilization of the square structure by 0.0255 Ha (16.0 kcal mol^{-1}), interference contributions counteract this difference by 0.0371 Ha (23.3 kcal mol^{-1}). This indicates that covalent effects tend to stabilize the system as it distorts by a second-order Jahn–Teller effect.

Table 2 shows the interference energy contribution of each set of chemical bonds in the square and rectangular cyclobutadienes, as well as in other hydrocarbons that have been studied previously.[58,61] The E[I] term of the C–H bonds is the same for all cyclobutadiene structures (−87.4 kcal mol^{-1}), and is similar to the same type of chemical bond in different hydrocarbons. Concerning the (C–C)σ bond, the interference contribution is, as expected, the same for both square states, but slightly less negative for the longer (C–C)σ bonds in the rectangular geometry.

The critical difference between the systems comes from the π space. Taking ethylene as a reference for a (C–C)π bond, one should expect that if the π interference energy of *trans*-butadiene was composed exclusively of the constructive interference between the carbon p-like orbitals participating in the π bond, its value would be −98.0 kcal mol^{-1}, twice that of ethylene. However, other orbital pairings in the π space tend to destabilize the system by about 16.8 kcal mol^{-1}. For the benzene

Table 1. Energy partitioning (in Ha) of the extreme points of the lowest singlet and triplet potential energy surfaces of cyclobutadiene.

	$^1B_{1g}$ (D_{4h})	$^3A_{2g}$ (D_{4h})	^1A_g (D_{2h})
E[tot]	−153.8200	−153.8039	−153.8316
E[ref]	−151.2915	−151.0058	−151.2477
$E[x]$	−1.3786	−1.3758	−1.3969
E[I]	−1.1567	−1.1829	−1.1944
E[II]	0.0068	−0.2393	0.0074

Table 2. Interference energy (E[I],in kcal mol^{-1}) of the chemical bonds of the lowest singlet and triplet states of cyclobutadiene.

	(C–H)σ	(C–C)σ	π space
$^1B_{1g}$ (D_{4h})	−87.4	−92.7	−5.4
$^3A_{2g}$ (D_{4h})	−87.5	−92.8	−21.4
^1A_g (D_{2h})	−87.4	−90.4; −92.7	−33.6
ethylene[a]	−86.3	−91.8	−49.0
trans-butadiene[a]	−86.9; −87.3	−92.3; −93.0	−81.2
benzene (D_{6h})[b]	−87.8	−93.4	−111.3

[a] Ref. [60]; [b] Ref. [57]

molecule, besides the destructive interference terms arising from nonadjacent p-like orbital pairs, there is another fundamental difference between the system and ethylene. The interference term between a p-like orbital and each one of its adjacent p-like orbitals is -23.0 kcal mol^{-1}, which is 26.0 kcal mol^{-1} higher in energy than the same contribution for ethylene. This reflects the fact that the π space of benzene is composed of a six center–six electron (6c–6e) chemical bond, as described elsewhere.[58] For the three cyclobutadiene structures, the total π interference is smaller than the (C–C)π interference energy of ethylene. This somewhat reflects the destabilizing nature of the π space of the system, which will be further analyzed in detail in Section 2.3.

The interference contribution between orbital pairs of the π space of the selected states of cyclobutadiene is shown in Table 3. For the rectangular X^1A_g state, the interference term $\phi_{C1}\phi_{C2}$, between orbitals centered on atoms C1 and C2, stabilizes the system by -49.5 kcal mol^{-1}, a value comparable with that of the ethylene π bond. However, as in the case of butadiene, in the π space there are also destructive interference terms, arising from orbital pairings not associated with the formation of the double bonds. These destabilizing terms are strong enough to make the overall π interference contribution of the four-electron system to be smaller than one two-electron π bond of ethylene. Therefore, the π space of the X^1A_g state could be described as composed by two alternating 2c–2e π bonds.

For the square singlet state, the situation is rather different from the previous case. The interference term that comes from each pairing of two adjacent orbitals is exactly the same, and

Table 3. Interference Energy partitioning [kcal mol^{-1}] of the π space of the lowest singlet and triplet states of cyclobutadiene into orbital pairs contribution.

	$^1B_{1g}$ (D_{4h})	$^3A_{2g}$ (D_{4h})	^1A_g (D_{2h})
Localized Orbitals			
$\phi_{C1}\phi_{C2}$	−13.9	–	−49.5
$\phi_{C2}\phi_{C3}$	−13.9	–	15.5
$\phi_{C1}\phi_{C3}$	25.1	–	17.2
Antipair Orbitals			
$\phi_{++,a}\phi_{++,b}$	–	−21.4	–
$\phi_{+-,a}\phi_{+-,b}$	–	0.0	–
$\phi_{++,a}\phi_{+-,b}$	–	0.0	–
$\phi_{+-,a}\phi_{++,b}$	–	0.0	–

corresponds to a stabilization of -13.9 kcal mol^{-1} per pair. In contrast, each nonadjacent term contributes to the destabilization of the system by 25.1 kcal mol^{-1}. This energy profile shows remarkable similarities with the benzene case. However, the energy values involved are very different. The small constructive interference contribution from adjacent orbital pairs and the particularly high destructive interference from the nonadjacent pairs are responsible for the overall π interference contribution of the square cyclobutadiene being just 5.4 kcal mol^{-1}. Thus, the π space of the X^1B_{1g} state could be described as being composed of a weak 4c–4e π bond.

Finally, for the square triplet state, contrasting features are also found for the interference contribution between the π space orbitals pairs. In this case, all contributions are zero, except for the pair of orbitals $\phi_{++,a}$ and $\phi_{++,b}$. The constructive interference contribution arising from this pair is -21.4 kcal mol^{-1}, and this leads to a very different bonding profile for the triplet square state. As at the spin-coupled level the orbitals are mono-occupied, the π space covalent contribution comes solely from two of the orbitals that comprise the four carbon centers. Therefore, it is possible to suggest that the π space of the $^3A_{2g}$ state could be described as being composed of a 4c–2e π bond, which is stronger than the bonding profile of the singlet square state, whereas the other two electrons are coupled in a triplet.

2.2. Automerization Reaction Path

Figure 2 shows the automerization reaction pathway from the square geometry ($\vec{Q}=0$) to the rectangle global minimum structures ($\vec{Q}=\pm1.0$) by applying the GPF-EP methodology along the automerization vector. In Figure 2a, the total electronic energy for the lowest singlet and triplet states is shown. As discussed in Section 2.1, the singlet–triplet gap and the automerization barrier are in agreement with previous studies.

Figure 2b shows the interference contribution of the singlet and triplet states along the automerization vector. For the triplet state, the interference contribution to stabilization diminishes as the geometry is distorted from the triplet minimum square structure. For the singlet state, there is discontinuity after the D_{4h} symmetry is broken, and the interference contribution reaches its maximum positive value of ≈10 kcal mol^{-1}. After the discontinuity, the π interference energy starts to stabilize the system as the Jahn–Teller distortion increases. At $\vec{Q}=\pm0.3$, the π interference contribution reaches zero, and changes sign subsequently. At $\vec{Q}=\pm0.7$, the π interference contribution from both states is the same (≈20 kcal mol^{-1}). Finally, at $\vec{Q}=\pm1.0$, it reaches the value of 33.6 kcal mol^{-1} (Table 2). This result reflects the trend of the π space to lower the interference energy towards the distortion to an alternating π bonding structure, as shown in previous studies.[36]

Figure 2c shows that the origin of the discontinuity observed in the π interference energy of the singlet state comes solely from the nonadjacent orbital pairs. At the D_{4h} symmetry, the destructive interference that comes from these pairs is smaller than those calculated at points in the vicinity. This discontinuity has its origin in the change of spin-coupling at the D_{4h} symmetry, leading to a discontinuous change in orbital shape. The discontinuity is a marker of significant change in the bonding profile after a symmetry break in the singlet state of cyclobutadiene, and is consistent with the results from Section 2.1.

Figure 3 shows the interference density plots in the π space for the singlet cyclobutadiene along the automerization reaction. The blue curves show regions in which the electron density is increasing, due to the interference effect, whereas the red curves indicate regions in which there is a removal of electron density by the interference effect. At $\vec{Q}=0$, the interfer-

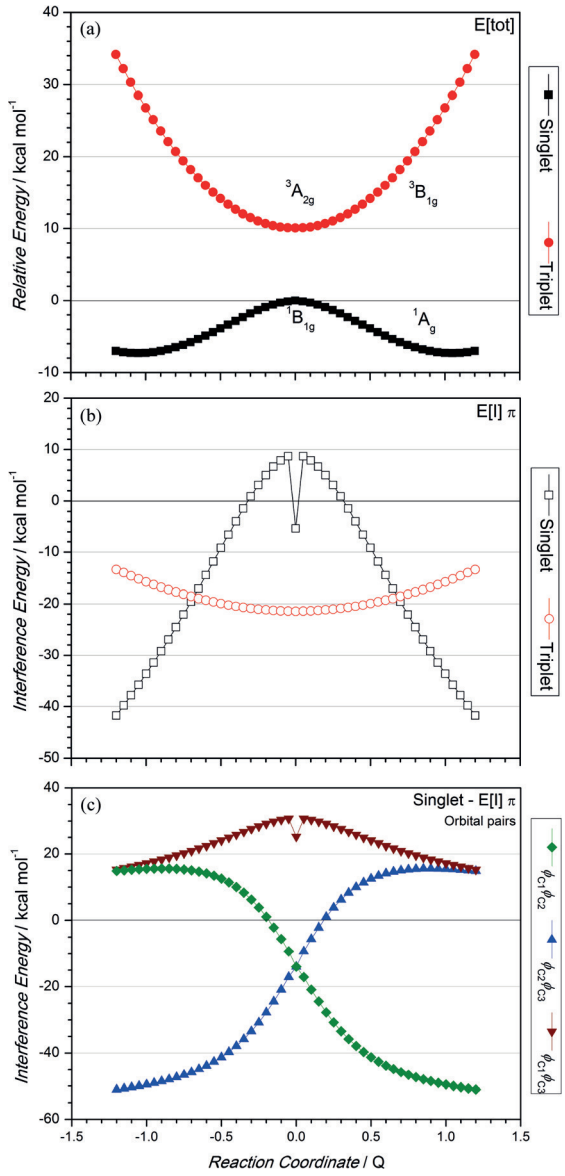

Figure 2. Energy partitioning of the lowest singlet and triplet states of cyclobutadiene along the automerization reaction coordinate. a) E[tot]. b) E[I]π. c) Interference contribution of each π orbital pair of the singlet state.

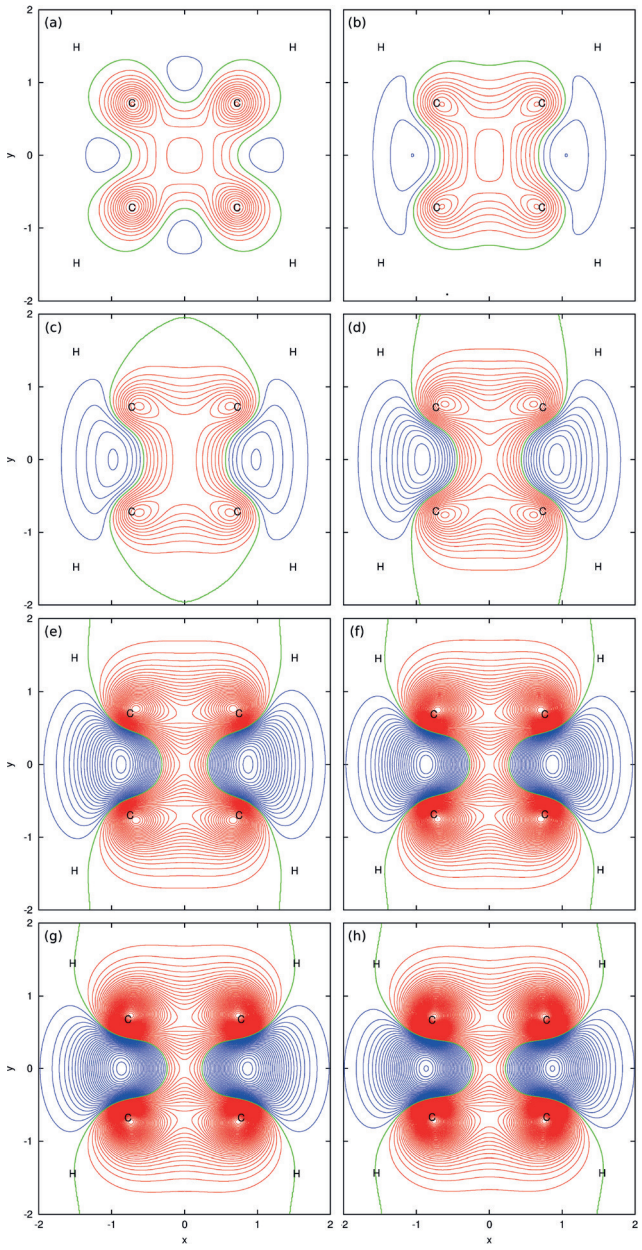

Figure 3. Interference density plots (z = 0.3 Å) of the π space along the automerization coordinate of the X^1B_{1g} state. a) $\vec{Q}=0$. b) $\vec{Q}=0.05$. c) $\vec{Q}=0.10$. d) $\vec{Q}=0.20$. e) $\vec{Q}=0.50$. (f) $\vec{Q}=0.75$. g) $\vec{Q}=1.0$. h) $\vec{Q}=1.2$.

ence effect removes electron density from around the carbon nuclei and equally increases electron density at the four C–C bonding centers. The result is consistent with the conclusion that the π space of the singlet square state is formed by a 4c–4e chemical bond. After the symmetry break, even in the vicinity of the square geometry, the electron density increases only at the two bonding centers in which the carbon atoms are closer, which suggests an abrupt change of the bonding pattern to form two 2c–2e π chemical bonds.

Figure 4 shows the interference density plots in the π space for the triplet cyclobutadiene along the automerization reaction. At $\vec{Q}=0$, as in the previous case, the interference effect increases electron density at the four C–C bonding centers in an equivalent manner. However, the same trend is observed when only the $\phi_{+,a}$ and the $\phi_{++,b}$ orbitals are considered, which is consistent to the 4c–2e bonding pattern. After geometry distortion, the interference effect removes electron density from the carbon centers that are approaching and increases electron density at the other two bonding centers. This means that the bonding structure changes, but there is no formation of π bonds in the rectangular structure of the triplet state.

2.3. Gas-phase Decomposition of Cyclobutadiene

In this section, the interference contribution is analyzed along the main decomposition reaction path of cyclobutadiene in the gas phase. At a pressure of 0.1 Torr, the lifetime of cyclobutadiene is merely 2 ms, and the main products are benzene and acetylene, following the reaction in Figure 5.[2] At the level

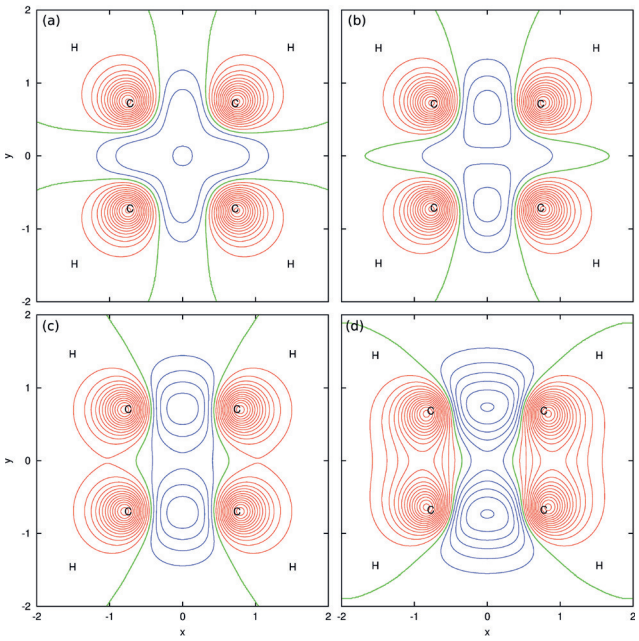

Figure 4. Interference density plots ($z=0.3$ Å) of the π space along the automerization coordinate of the $^3A_{2g}$ state. (a) $\vec{Q}=0.0$. (b) $\vec{Q}=0.20$. (c) $\vec{Q}=0.50$. (d) $\vec{Q}=1.0$.

of calculation used in this work, the ΔE without zero-point correction is -116.8 kcal mol^{-1}.

Assuming that the (C–C)σ and C–H bonds are of the same nature and that the (C–C)π bonds of the molecules are entirely equivalent to the (C–C)π bond of ethylene, the overall energetics could be naively described as the transformation of a (C–C)σ into a (C–C)π bond. As shown in Table 2, the interference energy of a (C–C)σ bond is more negative than that of a (C–C)π bond. One would end up concluding that the interference effect contributes to the stabilization of cyclobutadiene along the reaction pathway.

However, there are critical differences in the π space of the mentioned systems, which must be considered to obtain the correct picture. It is necessary to calculate an average interference energy value for each pair of electrons involved in the π

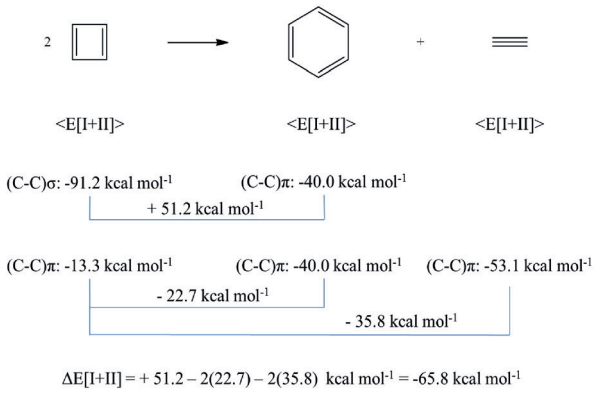

Figure 5. Interference energy contribution for the gas-phase decomposition reaction of cyclobutadiene.

bonding of the molecules. This can be achieved by taking the total interference energy (E[I + II]) of the π space and dividing it by the number of formal π bonds. These average values were used to estimate the contribution of the π space of cyclobutadiene to its destabilization, and to compare with strain effects. As shown in a previous study for cyclopropane, the ring torsion affects the quasiclassical energy significantly more than the interference counterpart.[63]

Figure 5 shows the total interference energy (including the second-order interference correction) contribution by using the average values of (C–C)σ and (C–C)π, and assuming that the interference energy of the C–H bonds are equal. The value obtained for the ΔE[I + II] is -65.8 kcal mol^{-1}. It can be concluded that, although strain effects are nonnegligible, the unstable nature of cyclobutadiene is dominated by covalent effects associated with the π space.

3. Conclusions

In this work, new insights concerning the chemical structure of the lowest energy singlet and triplet states of cyclobutadiene with a square geometry were reported. GPF-EP analysis showed that the π space of the $^1B_{1g}$ state is composed of a weak 4c–4e bond. This multicenter bonding character shows similarities to the benzene molecule, which has a 6c–6e π bond. However, the π interference contribution to the stability of cyclobutadiene is significantly smaller than in benzene. The implication is that the formation of multicenter bonds does not translate into a tendency for higher point-group symmetry geometries. Even so, the interference profile is heavily influenced by the spin couplings and can be used to determine the influence of the multicenter bond on the distortivity of molecules. This becomes evident when comparing the total interference contribution (E[I + II]) to the π distortivity of cyclobutadiene (28.2 kcal mol^{-1}) and benzene (7.5 kcal mol^{-1}).[58]

For the $^3A_{2g}$ square state, the GPF-EP analysis revealed the presence of a 4c–2e π bond, along with two triplet-coupled electrons. The contribution of the π interference to the stability of the system is higher than in the singlet case. To the best of our knowledge, this is the first time in which this type of bonding has been related to cyclobutadiene. The shape of the π orbitals, named antipair orbitals, and the interference analysis in the π space show that the system bears no relation with benzene or other aromatic compounds. This suggests that the so-called triplet aromaticity concept is, at least for cyclobutadiene, somewhat misleading.

A simple analysis of the interference contribution to the thermodynamics of the gas-phase decomposition of cyclobutadiene was also discussed. It was shown that, although strain effects were found to be nonnegligible, the thermodynamics of the main decomposition pathway of cyclobutadiene in the gas-phase is dominated by the π space interference.

Finally, the different mechanisms for maintaining the D_{6h} structure of benzene and the D_{2h} structure of cyclobutadiene should be reinforced. For both cases, the π distortivity tends to break the multicenter bonding, leading to the formation of 2c–2e π bonds. In benzene, this effect is counterbalanced

slightly by covalent effects related to the (C–C)σ bonds, and mainly by quasiclassical contributions to the energy.[58] In contrast, the interference contribution significantly stabilizes the cyclobutadiene molecule, as it follows the second-order Jahn–Teller distortion. Therefore, the highly symmetric D_{6h} structure of benzene is quasiclassical in nature, whereas covalent effects related to the π space are responsible for the alternating π-bond structure of cyclobutadiene.

Acknowledgements

The authors acknowledge Conselho Nacional de Desenvolvimento Científico e Tecnológico (CNPq), Coordenação de Aperfeiçoamento de Pessoal de Nível Superior (CAPES) and Fundação de Amparo à Pesquisa do Estado do Rio de Janeiro (FAPERJ) for financial support.

Keywords: ab intio calculations · bond theory · chemical bonds · cyclobutadiene · quantum interference

[1] G. F. Emerson, L. Watts, R. Pettit, *J. Am. Chem. Soc.* **1965**, *87*, 131 – 133.
[2] W. J. R. Tyerman, M. Kato, P. Kebarle, S. Masamune, O. P. Strausz, H. E. Gunning, *Chem. Commun.* **1967**, 497.
[3] G. Maier, H.-G. Hartan, T. Sayrac, *Angew. Chem. Int. Ed. Engl.* **1976**, *15*, 226 – 228; *Angew. Chem.* **1976**, *88*, 252 – 253.
[4] S. Masamune, F. A. Souto-Bachiller, T. Machiguchi, J. E. Bertie, *J. Am. Chem. Soc.* **1978**, *100*, 4889 – 4891.
[5] D. W. Whitman, B. K. Carpenter, *J. Am. Chem. Soc.* **1980**, *102*, 4272 – 4274.
[6] J. Kreile, N. Münzel, A. Schweig, H. Specht, *Chem. Phys. Lett.* **1986**, *124*, 140 – 146.
[7] A. M. Orendt, B. R. Arnold, J. G. Radziszewski, J. C. Facelli, K. D. Malsch, H. Strub, D. M. Grant, J. Michl, *J. Am. Chem. Soc.* **1988**, *110*, 2648 – 2650.
[8] B. R. Arnold, J. Michl, *J. Phys. Chem.* **1993**, *97*, 13348 – 13354.
[9] A. A. Deniz, *Science* **1999**, *286*, 1119 – 1122.
[10] A. Fattahi, L. Lis, Z. Tian, S. R. Kass, *Angew. Chem. Int. Ed.* **2006**, *45*, 4984 – 4988; *Angew. Chem.* **2006**, *118*, 5106 – 5110.
[11] R. J. Buenker, *J. Chem. Phys.* **1968**, *48*, 354.
[12] N. C. Baird, *J. Am. Chem. Soc.* **1972**, *94*, 4941 – 4948.
[13] M. J. S. Dewar, A. Komornicki, *J. Am. Chem. Soc.* **1977**, *99*, 6174 – 6179.
[14] H. Kollmar, V. Staemmler, *J. Am. Chem. Soc.* **1977**, *99*, 3583 – 3587.
[15] J. A. Jafri, M. D. Newton, *J. Am. Chem. Soc.* **1978**, *100*, 5012 – 5017.
[16] W. T. Borden, E. R. Davidson, P. Hart, *J. Am. Chem. Soc.* **1978**, *100*, 388 – 392.
[17] F. Fratev, V. Monev, R. Janoschek, *Tetrahedron* **1982**, *38*, 2929 – 2932.
[18] B. A. Hess, P. Carsky, L. J. Schaad, *J. Am. Chem. Soc.* **1983**, *105*, 695 – 701.
[19] S. S. Shaik, P. C. Hiberty, J. M. Lefour, G. Ohanessian, *J. Am. Chem. Soc.* **1987**, *109*, 363 – 374.
[20] C. H. Martin, R. L. Graham, K. F. Freed, *J. Chem. Phys.* **1993**, *99*, 7833.
[21] A. Balková, R. J. Bartlett, *J. Chem. Phys.* **1994**, *101*, 8972.
[22] Y. Mo, W. Wu, Q. Zhang, *J. Phys. Chem.* **1994**, *98*, 10048 – 10053.
[23] M. N. Glukhovtsev, S. Laiter, A. Pross, *J. Phys. Chem.* **1995**, *99*, 6828 – 6831.
[24] M. Filatov, S. Shaik, *J. Chem. Phys.* **1999**, *110*, 116 – 125.
[25] N. Allinger, C. Gilardeau, L. Chow, *Tetrahedron* **1968**, *24*, 2401 – 2406.
[26] S. C. Wright, D. L. Cooper, J. Gerratt, M. Raimondi, *J. Phys. Chem.* **1992**, *96*, 7943 – 7952.
[27] A. F. Voter, W. A. Goddard, *J. Am. Chem. Soc.* **1986**, *108*, 2830 – 2837.
[28] S. Shaik, A. Shurki, D. Danovich, P. C. Hiberty, *Chem. Rev.* **2001**, *101*, 1501 – 1540.
[29] Y. Shiota, M. Kondo, K. Yoshizawa, *J. Chem. Phys.* **2001**, *115*, 9243 – 9254.
[30] C. H. Suresh, N. Koga, *J. Org. Chem.* **2002**, *67*, 1965 – 1968.
[31] F. Dijkstra, J. H. Van Lenthe, R. W. A. Havenith, L. W. Jenneskens, *Int. J. Quantum Chem.* **2003**, *91*, 566 – 574.
[32] S. V. Levchenko, A. I. Krylov, *J. Chem. Phys.* **2004**, *120*, 175 – 185.
[33] B. Kovačević, D. Barić, Z. B. Maksić, T. Müller, *J. Phys. Chem. A* **2004**, *108*, 9126 – 9133.
[34] M. Eckert-Maksić, M. Vazdar, M. Barbatti, H. Lischka, Z. B. Maksić, *J. Chem. Phys.* **2006**, *125*, 64310.
[35] Y. Mo, P. v. R. Schleyer, *Chem. Eur. J.* **2006**, *12*, 2009 – 2020.
[36] S. C. A. H. Pierrefixe, F. M. Bickelhaupt, *Chem. Eur. J.* **2007**, *13*, 6321 – 6328.
[37] L. Watts, J. D. Fitzpatrick, R. Pettit, *J. Am. Chem. Soc.* **1965**, *87*, 3253 – 3254.
[38] M. J. S. Dewar, G. J. Gleicher, *J. Am. Chem. Soc.* **1965**, *87*, 3255 – 3256.
[39] P. C. Reeves, J. Henery, R. Pettit, *J. Am. Chem. Soc.* **1969**, *91*, 5888 – 5890.
[40] P. C. Reeves, T. Devon, R. Pettit, *J. Am. Chem. Soc.* **1969**, *91*, 5890 – 5891.
[41] R. Breslow, R. Grubbs, S. Murahashi, *J. Am. Chem. Soc.* **1970**, *92*, 4139 – 4140.
[42] B. Hess, L. Schaad, *Tetrahedron Lett.* **1972**, *13*, 5113 – 5116.
[43] G. Hohlneicher, L. Packschies, J. Weber, *Phys. Chem. Chem. Phys.* **2007**, *9*, 2517 – 2530.
[44] P. B. Karadakov, *J. Phys. Chem. A* **2008**, *112*, 7303 – 7309.
[45] J. I.-C. Wu, Y. Mo, F. A. Evangelista, P. v. R. Schleyer, *Chem. Commun.* **2012**, *48*, 8437 – 8439.
[46] M. P. Cava, M. J. Mitchell, *Cyclobutadiene and Related Compounds*, Academic Press, New York, **1967**, pp. 1 – 503.
[47] T. Bally, S. Masamune, *Tetrahedron* **1980**, *36*, 343 – 370.
[48] H. Kollmar, V. Staemmler, *Theor. Chim. Acta* **1978**, *48*, 223 – 239.
[49] G. A. Gallup, *J. Chem. Phys.* **1987**, *86*, 4018.
[50] D. W. Whitman, B. K. Carpenter, *J. Am. Chem. Soc.* **1982**, *104*, 6473 – 6474.
[51] B. K. Carpenter, *J. Am. Chem. Soc.* **1983**, *105*, 1700 – 1701.
[52] M. J. S. Dewar, K. M. Merz, J. J. P. Stewart, *J. Am. Chem. Soc.* **1984**, *106*, 4040 – 4041.
[53] M. J. Huang, M. Wolfsberg, *J. Am. Chem. Soc.* **1984**, *106*, 4039 – 4040.
[54] P. Carsky, R. J. Bartlett, G. Fitzgerald, V. Spirko, *Carbon* **1988**, *89*, 3008 – 3015.
[55] B. R. Arnold, J. G. Radziszewski, A. Campion, S. S. Perry, J. Michl, *J. Am. Chem. Soc.* **1991**, *113*, 692 – 694.
[56] R. G. Pearson, *J. Am. Chem. Soc.* **1969**, *91*, 4947 – 4955.
[57] R. S. Berry, *J. Chem. Phys.* **1961**, *35*, 2253.
[58] T. M. Cardozo, F. Fantuzzi, M. A. C. Nascimento, *Phys. Chem. Chem. Phys.* **2014**, *16*, 11024 – 11030.
[59] T. M. Cardozo, M. A. C. Nascimento, *J. Chem. Phys.* **2009**, *130*, 104102.
[60] T. M. Cardozo, M. A. C. Nascimento, *J. Phys. Chem. A* **2009**, *113*, 12541 – 12548.
[61] T. M. Cardozo, G. Nascimento Freitas, M. A. C. Nascimento, *J. Phys. Chem. A* **2010**, *114*, 8798 – 8805.
[62] F. Fantuzzi, T. M. Cardozo, M. A. C. Nascimento, *Phys. Chem. Chem. Phys.* **2012**, *14*, 5479 – 5488.
[63] F. S. Vieira, F. Fantuzzi, T. M. Cardozo, M. A. C. Nascimento, *J. Phys. Chem. A* **2013**, *117*, 4025 – 4034.
[64] F. Fantuzzi, M. A. C. Nascimento, *J. Chem. Theory Comput.* **2014**, *10*, 2322 – 2332.
[65] F. Fantuzzi, T. M. Cardozo, M. A. C. Nascimento, *J. Phys. Chem. A* **2015**, *119*, 5335 – 5343.
[66] P. Siegbahn, A. Heiberg, B. Roos, B. Levy, *Phys. Scr.* **1980**, *21*, 323 – 327.
[67] B. O. Roos, P. R. Taylor, P. E. Sigbahn, *Chem. Phys.* **1980**, *48*, 157 – 173.
[68] P. E. M. Siegbahn, *J. Chem. Phys.* **1981**, *74*, 2384.
[69] T. H. Dunning, *J. Chem. Phys.* **1989**, *90*, 1007.
[70] K. Ruedenberg, *Rev. Mod. Phys.* **1962**, *34*, 326 – 376.
[71] R. McWeeny, *Proc. R. Soc. London Ser. A* **1959**, *253*, 242 – 259.
[72] M. W. Schmidt, K. K. Baldridge, J. A. Boatz, S. T. Elbert, M. S. Gordon, J. H. Jensen, S. Koseki, N. Matsunaga, K. A. Nguyen, S. Su, T. L. Windus, M. Dupuis, J. A. Montgomery, *J. Comput. Chem.* **1993**, *14*, 1347 – 1363.
[73] J. Li, R. McWeeny, *Int. J. Quantum Chem.* **2002**, *89*, 208 – 216.
[74] R. McWeeny, *Theor. Chim. Acta* **1988**, *73*, 115 – 122.

Manuscript received: October 16, 2015
Accepted Article published: November 19, 2015
Final Article published: December 3, 2015